# Visualization of G-quadruplexes by using a BODIPY-labeled macrocyclic heptaoxazole†

**Masayuki Tera,[a] Keisuke Iida,[a] Kazunori Ikebukuro,[a] Hiroyuki Seimiya,[b] Kazuo Shin-ya[c] and Kazuo Nagasawa*[a]**

***Received 2nd February 2010, Accepted 30th March 2010***
***First published as an Advance Article on the web 22nd April 2010***
**DOI: 10.1039/c002117b**



A BODIPY-labeled macrocyclic heptaoxazole, L1BOD-7OTD, was developed as a fluorescent ligand for G-quadruplexes. The results of the study show that L1BOD-7OTD both selectively induces the formation of intramolecular G-quadruplexes from some G-quadruplex forming oligonucleotides (GFOs). In addition, the labelled macrocyclic heptaozaxole strongly binds to and stabilizes intramolecular G-quadruplexes. Moreover, this substance can be used to directly visualize the G-quadruplexes in the form of green fluorescence. Finally, the possibility that G-quadruplexes form in the cells was demonstrated by using of L1BOD-7OTD.

## Introduction

G-quadruplexes, which are one of the non B-DNA forms, are known to exist in telomeres at the ends of chromosomes, as well as in promoter regions of some oncogenes *in vitro*.[1] These G-quadruplexes can have different topological forms with characteristic biological activities, depending upon the class of monovalent cations they possess or their precise DNA sequence.[2] For example, in the presence of sodium and/or potassium ions single-stranded telomeric DNA can exist in more than three conformations including antiparallel, parallel, and antiparallel–parallel mixed types.[3] It has been reported that these structures induce apoptosis of cancer cells by promoting the dissociation of Pot1 and/or TRF2 from the t-loop domain in telomeric DNA.[4] In addition, it has been suggested that G-quadruplex structures in promoter regions of oncogenes is involved in regulating transcriptional activity. Although only a few G-quadruplexes have been described so far, bioinformatic analysis has led to the prediction that G-quadruplex forming motifs that are expected to play critical roles in various biological phenomena are present in promoter regions of over 40% of human genes.[5] In addition, G-quadruplexes have recently been utilized for bioengineering applications in the form of aptamers, which are a class of artificial functional oligonucleotides that are surrogate antibody candidates.[6] For example, the thrombin aptamer, containing fifteen guanines that forms a chair-like antiparallel intramolecular G-quadruplex, has been used as an anticoagulant agent owing to its strong binding affinity for the thrombin protein (nanomolar level $IC_{50}$).[7]

Since they have a variety of biological functions and are expected to be useful as bioengineering tools, G-quadruplexes hold great importance. As a result, the selection of new structures of this type in genes and artificial synthetic nucleotides is significant. Studies guided by these goals would be greatly aided by the availability of methods to visualize G-quadruplexes. Recently, fluorescent compounds, which interact with G-quadruplex structures and that bare chromophores or heavy-metal complexing sites, have been described.[8] One example comes from the work of Mergny and co-workers, which resulted in the development of bisquinolinium-thiazole orange conjugates that were used to visualize some classes of G-quadruplexes structures.[8a] In addition, a platinum(II) complex with dipyridophenazine was reported by Che and co-workers to serve as a luminescent probe for telomeric quadruplexes.[8b] On the other hand, a number of G-quadruplex ligands having significant biological activities including telomeric shortening and transcriptional control have been developed,[9] however, to our knowledge no studies have been carried out to apply those ligands to the fluorescent probes. Recently, we discovered that the macrocyclic heptaoxazole of 7OTD skeleton serves as a selective G-quadruplex binding ability.[10] Although L1H1-7OTD (**1**) stabilizes telomeric oligonucleotides in antiparallel structures, it does not interact with double-stranded DNA. Below, we describe the results of an effort that has led to the development of fluorescent labeled L1BOD-7OTD (**2**) and its application to the visualization of nucleotide sequences that form G-quadruplex structures in cell-free and cell-based assay systems.

## Results and discussion

The selection of the macrocyclic heptaoxazole skeleton of 7OTD as the foundation of new G-quadruplex complexing agents is based upon an analysis of the natural product telomestatin, a potent telomerase inhibitor that interacts with telomeric G-quadruplexes.[11] The results of earlier structure–activity relationship studies with side chain functional group containing derivatives (amino group of **1** in Fig. 1) showed that the 7OTD skeleton is as efficient as telomestatin in stabilizing representative

[a]*Department of Biotechnology and Life Science Faculty of Technology, Tokyo University of Agriculture and Technology (TUAT), Koganei, Tokyo 184-8588, Japan. E-mail: knaga@cc.tuat.ac.jp; Fax: +81-42-388-7295; Tel: +81-42-388-7295*
[b]*Cancer Chemotherapy Center, Japanese Foundation for Cancer Research, Koto-ku, Tokyo 135-8550, Japan*
[c]*Biological Information Research Center National Institute of Advanced Industrial Science and Technology, Koto-ku, Tokyo 135-0064, Japan*
† Electronic supplementary information (ESI) available: NMR spectra, excitation and emission spectrum, ESI-MS spectra, FP-titration and UV-melting assay. See DOI: 10.1039/c002117b

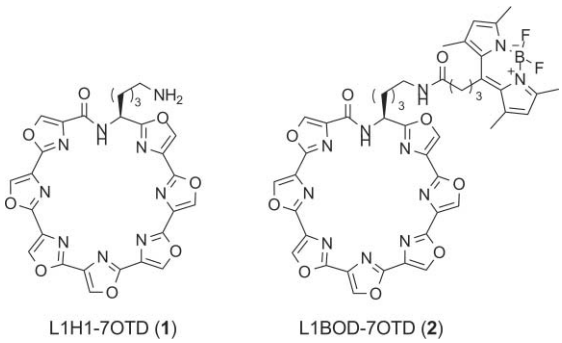


**Fig. 1** Molecular structure of L1H1-7OTD (**1**) and fluorescent labelled L1BOD-7OTD (**2**).

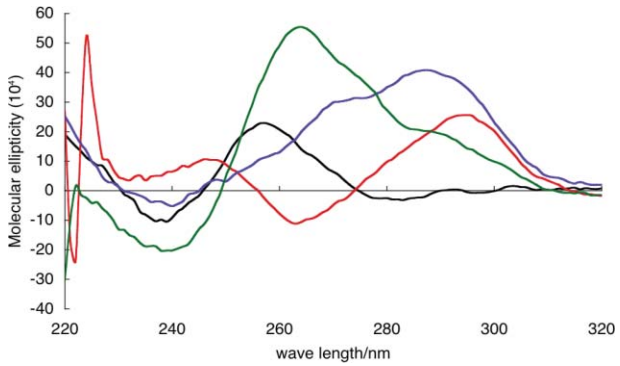


**Fig. 2** CD spectra of telo24 (10 μM) in Tris-HCl buffer (50 mM, pH 7.3) with 50 μM L1BDO-7OTD and/or 100 mM KCl. Black line: telo24 (no salt added); red line: telo24 + L1BOD-7OTD (no salt added); blue line: telo24 + KCl; green line: telo24 + KCl + L1BOD-7OTD.

G-quadruplex structures.[10a] These findings led to the design of a new fluorescent G-quadruplex binder, L1BOD-7OTD (**2**), which is a conjugate of the fluorophore BODIPY (4,4-difluoro-4-bora-3a,4a-diaza-*s*-indacene) and the macrocyclic heptaozaxole **1**, linked *via* an amide bond. Several advantageous properties drove the selection of BODIPY as the fluorophore. These include its high fluorescence quantum yield that is insensitive to pH and solvent polarity, and its narrow long-wavelength emission.[12]

L1BOD-7OTD (**2**) was synthesized starting with previously reported **1**. L1BOD-7OTD displays green fluorescence with wavelengths for its excitation and emission maxima of 502 and 512 nm, respectively (see ESI†). The ability of **2** to stabilize G-quadruplex structures was evaluated by means of circular dichroic (CD) analysis using telo24, a single-stranded telomeric oligonucleotide that is known to have a propensity for G-quadruplex formation (Fig. 2). Telo24 has a random structure in the absence of monovalent cations and/or G-quadruplex binders. Upon treatment of this telomeric oligonucleotide with **2**, the CD spectrum changes in a manner that gives rise to a positive peak at 292 nm and a negative peak at 262 nm. These characteristic spectral changes clearly show that **2** induces a conversion of the random structure of telo24 into an antiparallel G-quadruplex structure. Interestingly, in the presence of 100 mM KCl, L1BOD-7OTD promotes conversion of telo24 from an antiparallel-parallel mixed mode into a parallel mode structure.[13] Furthermore, induction and structural stabilization of G-quadruplex structure of telomeric DNA of flu-telo21 as well as the other four representative G-quadruplex forming oligonucleotides (GFOs) including flu-myc22, flu-bcl27, flu-kit21 and a thrombin aptamer of flu-thr20 by L1BOD-7OTD was quantitatively evaluated by fluorescence resonance energy transfer (FRET) melting assay using fluorescence-labeled, single-stranded oligonucleotide (Table 1).[14] The $\Delta T_{1/2}$ values of **2** at the concentration of 1 μM, which corresponds to 5 equivalents with respect to labeled oligonucleotides, are summarized in Table 2. Since the $\Delta T_{1/2}$ values of labeled GFOs were significantly increased in all cases, it was suggested that L1BOD-7OTD bound to GFOs and stablized the G-quadruplex structures.

The presence of selective interactions between L1BOD-7OTD (**2**) and the telomeric DNA sequence as well as visualization of the telomeric G-quadruplex structure were examined by using an electrophoresis mobility shift assay (EMSA), employing both telo24 and its duplex sequence of ds-telo24 (Fig. 3). In the presence of **2**, a green band ($\lambda_{ex}$ = 488 nm, 526 nm short pass filter) associated with the telo24 - L1BOD-7OTD complex

**Table 1** Single-stranded oligonucleotides used in this paper

| Oligomer name | Sequence |
|---|---|
| telo24 | 5′-TTAGGGTTAGGGTTAGGGTTAGGG-3′ |
| myc22 | 5′-GAGGGTGGGGAGGGTGGGGAAG-3′ |
| kit22 | 5′-AGGGAGGGCGCTGGGAGGAGGG-3′ |
| bcl27 | 5′-CGGGCGCGGGAGGAAGGGGGCGGGAGC-3′ |
| thr15 | 5′-GGTTGGTGTGGTTGG-3′ |
| telomut24 | 5′-TTAGAGTTAGAGTTAGAGTTAGGG-3′ |
| polyT24 | 5′-TTTTTTTTTTTTTTTTTTTTTTTT-3′ |
| stem-loop26 | 5′-TATAGCTATATTTTTTTATAGCTATA-3′ |
| flu-telo21 | FAM-5′-GGGTTAGGGTTAGGGTTAGGG-3′-TAMRA |
| flu-myc22 | FAM-5′-GAGGGTGGGGAGGGTGGGGAAG-3′-TAMRA |
| flu-kit21 | FAM-5′-GGGAGGGCGCTGGGAGGAGGG-3′-TAMRA |
| flu-bcl27 | FAM-5′- CGGGCGCGGGAGGAAGGGGGCGGGAGC-3′-TAMRA |
| flu-thr20 | FAM-5′- TTTTAGGTTGGTGTGGTTGG-3′-TAMRA |

**Table 2** $\Delta T_{1/2}$ at 1 μM L1BOD-7OTD (**2**) obtained by FRET melting assay[14]

| Oligomer name | flu-telo21 | flu-myc22 | flu-bcl27 | flu-kit21 | flu-thr20 |
|---|---|---|---|---|---|
| $\Delta T_{1/2}$ (°C) | 14.7 | 10.8 | 7.5 | 13.6 | 4.4 |



 

is observed with an intensity that varies in a dose dependent manner (Fig. 3a). The presence of oligonucleotide in this band was determined by treatment of the gel with Stains-all® which enables visualization of uncomplexed telo24 as a red band (Fig. 3b).[15] The results show that the amount of the telo24 G-quadruplex in the green band increases in a way that is directly proportional to the concentration of L1BOD-7OTD. In addition, randomly structured telo24 (red lower mobility band; Fig. 3b) decreases in a complementary manner. By using this method of analysis, the complex of telo24 with ligand **2** is directly observed as a green fluorescent band without the need for staining while the red band of lower mobility seen only by staining corresponds to the ligand-free nucleotide (Fig. 3c shows the merged image). In contrast, the EMSA analysis of mixtures of ds-telo24 with 2 shows that no green fluorescent band is produced (Fig. 3d) and only the red band for uncomplexed ds-telo24 exists even when higher concentrations of L1BOD-7OTD are present (Fig. 3e). The findings indicate that no interaction takes place between 2 and ds-telo24 and, as a result, that the interaction of 2 with G-quadruplex is selective and visualizable against double-stranded DNA.[16]

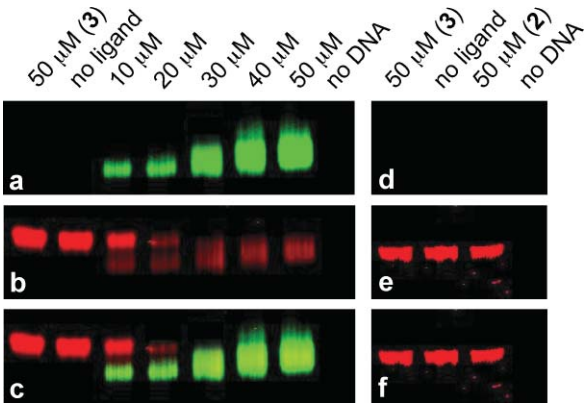


**Fig. 3** Visualization of the telo24 G-quadruplex by L1BOD-7OTD. Gel electrophoresis (12% native polyacrylamide, in 1 × TBE buffer, 4 °C) of 10 μM oligonucleotides (a–c: telo24, d–f: ds-telo24) in the presence of various concentrations of **2** (no salt added).[17a] a, d) All bands were detected using the 526 nm short pass filter. The gel was stained with b) Stains-all® and e) ethidium bromide then all bands were detected using the 580–640 nm band pass filter. c, f) Merged images of a and b or d and e. Compound **3**[17b] was used as a control for the BODIPY moiety of **2** (see ESI†).

The generality of the GFOs detecting system based on L1BOD-7OTD (**2**) was examined next. For this purpose, four representative GFOs, myc22, kit22, bcl27,[18] a thrombin aptamer of thr15, and three non-GFOs, stem-loop26 (stem-loop structure), polyT24, and telomut24 (single-stranded random structure), were employed. Mixtures of various concentrations (10–50 μM) of **2** and each of these substances was subjected to electrophoresis analysis. The results of EMSA analysis (Fig. 4) show that the G-quadruplex structures of myc22, kit22, bcl27 and thr15 are induced through high-affinity interactions with **2** and that the complexes are directly observed as green bands (Fig. 4a–d). In contrast, EMSA analysis shows that stem-loop26, polyT24 and telomut24 only show red bands even when a high concentration of **2** is present (Fig. 4e–g). Thus, **2** interacts in a highly selective manner with GFOs giving stabilized quadruplex structures that are visualized as green fluorescent bands.

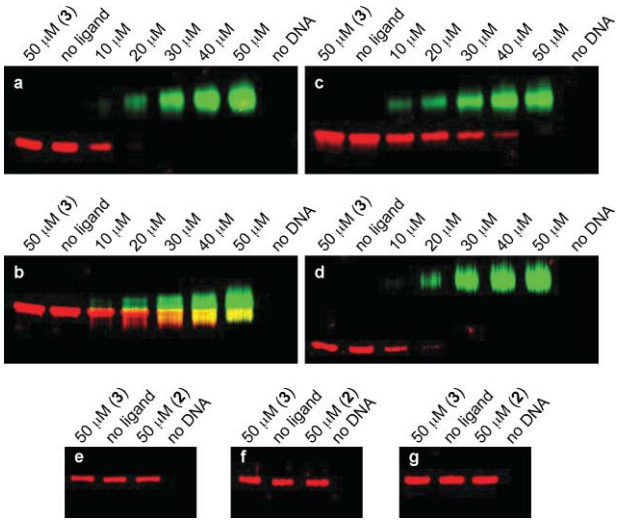


**Fig. 4** Gel electrophoresis (12% native polyacrylamide, in 1 × TBE buffer, 4 °C) of 10 μM GFOs (a: myc22, b: bcl27, c: kit22, d: thr15) and non-GFOs (e: polyT24, f: stem-loop26, g: telomut24) in the presence of various concentrations of **2** (no salt added).[17a] All merged images were obtained by 526 nm short pass filter (green band) and 580–640 nm band pass filter (red band) after staining by Stains-all®. Compound **3**[17b] was used as a control for the BODIPY moiety of **2**.

The binding stoichiometries of L1BOD-7OTD with GFOs were determined by using ESI-MS spectrometric analysis.[19] The mass spectra of mixtures of the five GFOs (telo24, myc22, kit22, bcl-27 and thr15) with L1BOD-7OTD in molar ratios of 1 : 4 are shown in Fig. 5. In all cases, mass peaks associated with both 1 : 1 and/or 1 : 2 complexes of GFOs and L1BOD-7OTD are detected (see ESI†).

To determine the apparent dissociation constants ($K_d$) of the complexes of **2** with the GFOs, fluorescent polarization (FP) titration measurements were made.[20] After incubating mixtures of 50 nM L1BOD-7OTD, 50 mM KCl, and various concentrations of the GFOs (0.1–400 nM) for 12 h, the FP values were determined at 25 °C. Since ESI-MS analysis had shown that L1BOD-7OTD and GFOs form 2 : 1 stoichiometric complexes, the FP-[GFOs] plots were fitted using nonlinear regression analysis (Fig. 6, Table 3).[21b] As the results in Table 3 show, L1BOD-7OTD was revealed to have potent dissociation constant toward G-quadruplexes with nanomolar level. In the cases of ds-telo24 and telomut24 (negative control), no interaction with **2** is observed (see ESI†) thus it appears that L1BOD-7OTD potently and selectively bound to G-quadruplexes.

Finally, cell-based G-quadruplex visualization was explored by using HeLa I.2.11 cells (Fig. 7). After treatment of living HeLa I.2.11 cells with 0.5 μM L1BOD-7OTD for 18 h,[22] they

**Table 3** Apparent dissociation constants ($K_d$) of L1BOD-7OTD (**2**) and GFOs measured by fluorescence polarization titration[21]

| Oligomer name | telo24 | myc22 | bcl27 | kit22 | thr15 |
|---|---|---|---|---|---|
| $K_d$ (nM) | 6.4 | 0.2 | 58 | 5.7 | 80 |

The $K_d$ values were calculated by following equation; $FP = FP_{max} \times (([L1BOD\text{-}7OTD] + [GFOs] + K_d) - (([L1BOD\text{-}7OTD] + [GFOs] + K_d)^2 - 4 \times [L1BOD\text{-}7OTD] \times [GFOs])^{1/2}) / (2 \times [L1BOD\text{-}7OTD])$[21a,b]

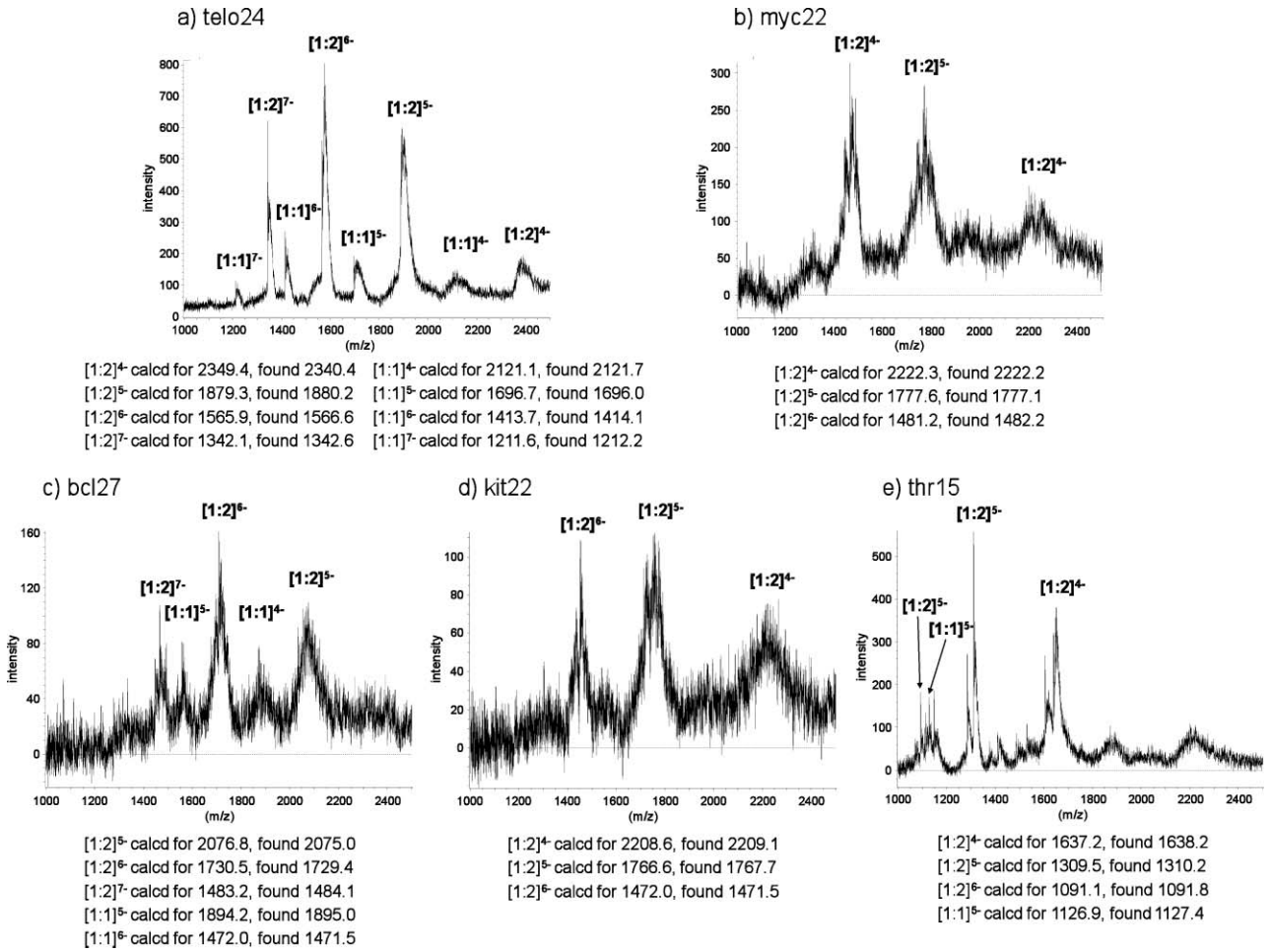


**Fig. 5** ESI-MS spectra of mixtures of L1BOD-7OTD (**2**) with the GFOs: (a) telo24, (b) myc22, (c) bcl27, (d) kit22 and (e) thr15. (see also ESI†).

were fixed by using paraformaldehyde and stained with DAPI to visualize nuclei (Fig. 7b). Analysis of microscope images show that green fluorescent foci, derived from L1BOD-7OTD, overlap with blue fluorescent foci associated with DAPI (Fig. 7c). The results demonstrate that L1BOD-7OTD permeates cell and nuclear membranes and localizes in the nuclei of the cells.[23]

## Conclusion

This investigation has led to the development of the fluorescence-labeled macrocyclic heptaoxazole L1BOD-7OTD (**2**), which serves as a novel fluorescent ligand for G-quadruplexes. The macrocyclic heptaoxazole selectively interacts with GFOs by inducing the formation of and stabilizing G-quadruplex structures. It is noteworthy that L1BOD-7OTD (**2**) also selectively interacts with an artificial G-quadruplex aptamer. Interactions of this fluorescent ligand with G-quadruplex structures in genes and artificial nucleotides can be directly visualized as a consequence of the green fluorescence of **2**. Moreover, the studies have demonstrated that this macrocyclic heptaoxazole ligand can be employed to visualize G-quadruplexes in cell-free and cell-based assay systems. Studies of the applications of the new methodology to the direct detection or selection of G-quadruplex forming motifs in genes and artificial nucleotide libraries are currently under way.

## Experimental

### Material and instruments for synthesis

Flash chromatography was performed by using Silica gel 60 (spherical, particle size 0.040 ~ 0.100 μm; Kanto). $^{1}$H and $^{13}$C NMR spectra were recorded on a JEOL JNM-ECX 400 instrument. The spectra are referenced internally to signals of the residual solvent $(CD_3)_2SO$ ($^{1}$H NMR; $\delta$ = 2.50 ppm, $^{13}$C NMR; $\delta$ = 39.5 ppm). Data for $^{1}$H NMR are recorded as follows: chemical shift (ppm), multiplicity (s, singlet; d, doublet; t, triplet; m, multiplet; br, broad), integration, coupling constant (Hz). Data for $^{13}$C NMR are reported in terms of chemical shifts (ppm). Mass spectra were recorded on a JEOL JMS-T100X spectrometer using an ESI-MS mode and methanol as solvent.

### Synthesis of L1BOD-7OTD (2)

To a solution of L1H1-7OTD (**1**) (26 mg, 37 μmol) in 1 : 4 $CH_2Cl_2$–THF (10 mL) was added the activated ester of BODIPY (see ESI†) (28 mg, 65.0 μmol), The resulting mixture was stirred at 70 °C for 48 h, and concentrated *in vacuo*, giving a residue, which was to subjected to chromatography on silica gel ($CHCl_3$–AcOEt–MeOH = 3 : 2 : 1) to give L1BOD-7OTD (**2**) as an orange solid (23 mg, 66%) with $a$ > 91% purity ($C_{18}$ reverse phase column,

 

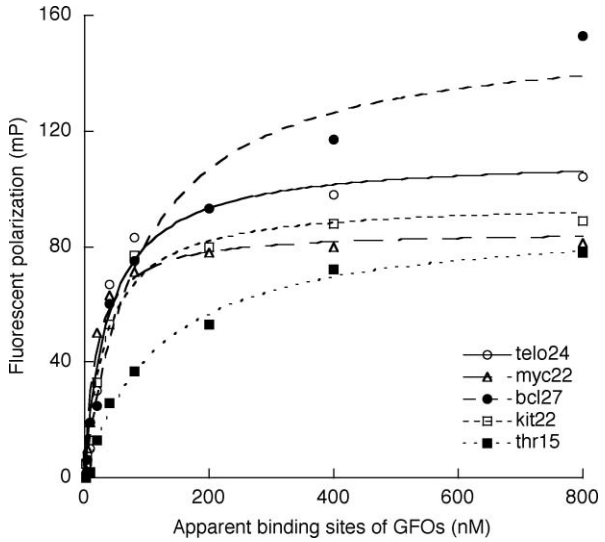


**Fig. 6** FP titrations of GFOs. L1BOD-7OTD (**2**) (50 nM) was incubated with various concentrations (1–400 nM) of the GFOs (open circle: telo24, open triangle: myc22, black circle: bcl27, open square: kit22, black square: thr15) at 25 °C for 12 h in the presence of 50 mM KCl, 5 mM Tris-HCl, pH 7.0 and 50% DMSO (v/v).[21c] The polarization associated with the emission of **2** was measured at 530 nm (excitation at 500 nm). The fluorescent polarization values are representative of five scans taken at 25 °C. All plots result from duplicate assays.

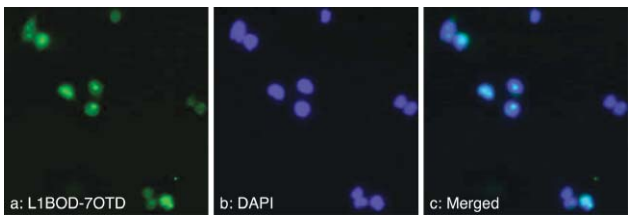


**Fig. 7** Fluorescence microscopic imaging of nuclei of fixed HeLa I.2.11 cells after 18 h treatment of L1BOD-7OTD (0.5 μM). a) L1BOD-7OTD fluorescent ($\lambda_{ex}$ = 502 nm, $\lambda_{em}$ = 512 nm). b) DAPI fluorescent ($\lambda_{ex}$ = 358 nm, $\lambda_{em}$ = 461 nm). c) Merged image of a and b.

with 70%MeOH-30%$H_2O$-0.1%TFA as mobile phase, monitored at 254 nm. See ESI†). TLC $R_f$ 0.5 (3 : 2 : 2 $CHCl_3$–EtOAc–MeOH). Spectral data for L1BOD-7OTD (**2**): $^1$H NMR (400 MHz, DMSO d-6) $\delta$ 9.06 (s, 1H), 9.00 (s, 1H), 8.99 (s, 1H), 8.90 (s, 1H), 8.85 (s, 1H), 8.78 (s, 1H), 8.63 (s, 1H), 8.41 (d, $J$ = 7.8 Hz, 1H), 8.14 (t, $J$ = 6.0 Hz, 1H), 6.12 (s, 2H), 5.56 (dt, $J$ = 4.6, 7.8 Hz, 1H), 3.03 (m, 1H), 2.85 (m, 1H), 2.67 (t, $J$ = 8.7 Hz, 2H), 2.43 (s, 6H), 2.16 (br, 9H), 1.88 (m, 1H), 1.63 (m, 2H), 1,32 (m, 2H), 1.02 (m, 1H), 0.82 (m, 1H); $^{13}$C NMR (100 MHz, DMSO d-6) $\delta$ 171.2, 163.6, 159.2, 155.8, 155.7, 155.5, 155.2, 154.8, 153.1, 145.9, 143.2, 140.6, 140.5, 139.9, 139.2, 138.9, 138.8, 136.1, 130.4, 129.8, 129.7, 129.6, 128.6, 121.5, 47.6, 35.4, 33.1, 29.0, 28.5, 27.9, 26.8, 21.0, 15.5, 14.1; HRMS (ESI, M+Na) calcd for $C_{44}H_{38}BF_2N_{11}O_9Na$ 936.2813, found 936.2768.

### Oligonucleotides

All pure oligonucleotides and fluorescent labeled ones were obtained from Sigma Genosys and dissolved in double-distilled water to be used without further purification.

### CD spectrometry

CD spectra were recorded on a JASCO-810 spectropolarimeter (Jasco, Easton, MD) using a quartz cell of 1-mm optical path length and an instrument scanning speed of 100 nm min$^{-1}$ with a response time of 1 s, and over a wavelength range of 220-320 nm. The CD titration experiment was performed by using a modification of the reported procedure.[10b] The GFOs of telo24 was dissolved in Tris-HCl buffer (50 mM, pH 7.6) and the solution was heated to 94 °C for 2 min, then slowly cooled to 25 °C. L1BOD-7OTD (**2**) was diluted from a 10 mM stock solution in 100% DMSO to a concentration of 1 mM with DMSO and sequentially added to the oligonucleotide samples. The DNA concentrations were 10 μM, and the CD spectra are representative of three averaged scans taken at 25 °C.

### FRET melting assay

FRET melting assay was performed using a modification of the reported procedure.[14] Briefly, The dual fluorescently labeled oligonucleotides were used in this protocol. The donor fluorophore was 6-carboxyfluorescein, FAM, and the acceptor fluorophore was 6-carboxytetramethylrhodamine, TAMRA. The oligonucleotides were initially dissolved as a 100 mM stock solution in MilliQ water; further dilutions were carried out in 60 mM each potassium chloride and cacodylate buffer (pH 7.4). Dual-labeled DNA was annealed at a concentration of 400 nM by heating at 95 °C for 2 min followed by cooling to room temperature. The various concentrations of L1BOD-7OTD were added into different samples, using a total reaction volume of 100 mL, with 200 nM of labeled oligonucleotide. Then the samples were incubated at 4 °C for overnight. Following experiments should keep the temperature procedure in real-time PCR and procedure was finished as following: 4 °C for 30 min, then a stepwise increase of 1 °C every minute from 4 °C to reach 99 °C. During the procedures, the intensity of FAM was measured after each stepwise.

### Electrophoresis mobility shift assay

EMSA was performed using a modification of the reported procedure.[10a] Briefly, a solution of telo24 oligonucleotide in Tris-HCl buffer (50 mM, pH 7.1) was heated at 94 °C for 2 min and then slowly cooled to 25 °C. Various concentrations of L1BOD-7OTD (**2**) in DMSO, prepared from a 5 mM stock solution, were added to the telo24 (10 μM) sample. After a 12 h incubation period, the samples were mixed with Ficol 400 solution (100 mg mL$^{-1}$), resolved on 12% native polyacrylamide gels in 1 × TBE buffer at 4 °C and stained with Stains-all® or ethidium bromide. The gels were scanned with a phosphorimager (Typhoon 8600, Molecular Dynamics) using 526 nm short pass and 580–640 band pass filters, respectively, in order to visualize the fluorescent areas.

### Fluorescent polarization titration

Fluorescent polarizations were recorded on a FP-715 (Jasco) using a quartz cell of 5-mm optical path length. The excitation wavelength was 500 nm and the emission wavelength was 530 nm. The G factor was determined from 0.7 μM L1BOD-7OTD in a 10 mM Tris-HCl and 100 mM KCl buffer, pH 7.3 (FP = 30 mP).

### ESI-MS spectrometry

All measurements were carried out on a JMS-T100LC AccuTOF (JEOL), using the electrospray ionization (ESI) source in negative mode, as described previously.[19] The measurement conditions and the sample preparation procedures were as follows: capillary needle voltage, −2.0 kV; ring lens voltage, −15 V; orifice 1 voltage, −75 V; orifice 2 voltage, 0 V; orifice 1 temperature, 80 °C; desolvation temperature, 80 °C; sample flow rate, 5 μL $min^{-1}$; All experiments were performed in 20 mM $NH_4OAc$ containing 10 μM of GFOs and 40 μM of **2**. Methanol (10%) was added just before injection. The role of methanol is to increase ion signals.

### Cell imaging

HeLa I.2.11 cells were grown in DMEM media supplemented with 10% FBS, 2 mM L-Glutamine, 100 units/mL of penicillin, 100 μg/mL streptomycin, and 1 mM Sodium pyruvate on 10 mm diameter cover slip for overnight. After being treated with L1BOD-7OTD (0.5 μM, 0.1% DMSO) for 18 h, the cells were fixed using 2% paraformaldehyde/PBS for 10 min and permeabilized with 0.5% NP-40/PBS. The nuclei were stained by using DAPI. The cells were imaged by using an inverted fluorescence microscope IX71 (Olympus) and a combination of excitation and emission filters (For DAPI: 330–385 nm excitation filter and 420 short pass filter were used and for L1BOD-7OTD: 490–505 nm excitation filter and 515–560 nm band pass filter were used.). The images of the cells were recorded using a computer-controlled CCD camera DP70 (Olympus).

## Acknowledgements

We thank Dr R. Saito (Toho University) and Dr K. Yamada (TUAT) for helpful discussion. This work was supported in part by the Novartis Foundation (Japan) for the Promotion of Science, a Grant-in-Aid for Exploratory Research (21655060) and a grant under the Industrial Technology Research Grant Program (01A04006b) from the New Energy and Industrial Technology Development Organization (NEDO) of Japan. M.T. and K. I. are grateful for a JSPS Research Fellowship for Young Scientists and a grant under the education program "Human Resource Development Program for Scientific Powerhouse" provided through TUAT.

## References

1 For recent reviews for the G-quadruplex structures in human gene promoter sequences, see: (*a*) Y. Qin and L. H. Hurley, *Biochimie*, 2008, **90**, 1149; (*b*) S. Neidle and G. N. Parkinson, *Biochimie*, 2008, **90**, 1184; (*c*) D. J. Patel, A. T. Phan and V. Kuryavyi, *Nucleic Acids Res.*, 2007, **35**, 7429G-quadruplex structure of c-kit promoter, see: (*d*) A. T. Phan, V. Kuryavyi, S. Burge, S. Neidle and D. J. Patel, *J. Am. Chem. Soc.*, 2007, **129**, 4386; (*e*) P. S. Shirude, B. Okumus, L. Ying, T. Ha and S. Balasubramanian, *J. Am. Chem. Soc.*, 2007, **129**, 7484; (*f*) A. K. Todd, S. M. Haider, G. N. Parkinson and S. Neidle, *Nucleic Acids Res.*, 2007, **35**, 5799In the case of bcl-2, see: (*g*) J. Dai, T. S. Dexheimer, D. Chen, M. Carver, A. Ambrus, R. A. Jones and D. Yang, *J. Am. Chem. Soc.*, 2006, **128**, 1096; (*h*) T. S. Dexheimer, D. Sun and L. H. Hurley, *J. Am. Chem. Soc.*, 2006, **128**, 5404; In the case of c-myc, see: T. Simonsson, P. Pecinka and M. Kubista, *Nucleic Acids Res.*, 1998, **26**, 1167.

2 Transcriptional regulation of c-kit, see: (*a*) M. Bejugam, S. Sewitz, P. S. Shirude, R. Rodriguez, R. Shahid and S. Balasubramanian, *J. Am. Chem. Soc.*, 2007, **129**, 12926c-myc transcription, see: (*b*) A. Siddiqui-Jain, C. L. Grand, D. J. Bearss and L. H. Hurley, *Proc. Natl. Acad. Sci. U. S. A.*, 2002, **99**, 11593bcl-2 transcription, see: (*c*) C. Douarre, D. Gomez, H. Morjani, J. M. Zahm, M. F. O'Donohue, L. Eddabra, P. Mailliet, J. F. Riou and C. Trentesaux, *Nucleic Acids Res.*, 2005, **33**, 2192.

3 In the presence of potassium cation, the telomeric G-quadruplex forms a parallel or antiparallel/parallel mixed type structure, see: (*a*) G. N. Parkinson, M. P. Lee and S. Neidle, *Nature*, 2002, **417**, 876; (*b*) D. J. Patel, A. T. Phan and V. Kuryavyi, *Nucleic Acids Res.*, 2007, **35**, 7429; (*c*) Y. Xu, Y. Noguchi and H. Sugiyama, *Bioorg. Med. Chem.*, 2006, **14**, 5584; (*d*) A. Ambrus, D. Cheng, J. Dai, T. Bialis, R. A. Jones and D. Yang, *Nucleic Acids Res.*, 2006, **34**, 2723; (*e*) J. Dai, C. Punchihewa, A. Ambrus, D. Chen, R. A. Jones and D. Yang, *Nucleic Acids Res.*, 2007, **35**, 2440In the presence of sodium cation, the telomeric G-quadruplex forms an antiparallel structure, see: (*f*) Y. Wang and D. J. Patel, *Structure*, 1993, **1**, 263.

4 (*a*) H. Tahara, K. Shin-ya, H. Seimiya, H. Yamada, T. Tsuruo and T. Ide, *Oncogene*, 2006, **25**, 1955; (*b*) D. Gomez, T. Wenner, B. Brassart, C. Douarre, M.-F. O'Donohue, V. E. Khoury, K. Shin-ya, H. Morjani, C. Trantesaux and J. F. Riou, *J. Biol. Chem.*, 2006, **281**, 38721.

5 (*a*) J. L. Huppert and S. Balasubramanian, *Nucleic Acids Res.*, 2006, **35**, 406; (*b*) V. K. Yadav, J. K. Abraham, P. Mani, R. Kulshrestha and S. Chowdhury, *Nucleic Acids Res.*, 2007, **36**(database), D381; (*c*) R. Zhang, Y. Lin and C. Zhang, *Nucleic Acids Res.*, 2007, **36**, D372.

6 For a recent review, see: G. Mayer, *Angew. Chem., Int. Ed.*, 2009, **48**, 2672.

7 R. F. Macaya, P. Schultze, F. W. Smith, J. A. Roe and J. Feigon, *Proc. Natl. Acad. Sci. U. S. A.*, 1993, **90**, 3745.

8 (*a*) P. Yang, A. D. Cian, M. P. Teulade-Fichou, J. L. Mergny and D. Monchaud, *Angew. Chem., Int. Ed.*, 2009, **48**, 2188; (*b*) D. L. Ma, C. M. Che and S. C. Yan, *J. Am. Chem. Soc.*, 2009, **131**, 1835; (*c*) Y. Hong, H. Xiong, J. W. Y. Lam, M. Haubler, J. Liu, Y. Yu, Y. Zhong, H. H. Y. Sung, I. D. Williams, K. S. Wong and B. Z. Tang, *Chem.–Eur. J.*, 2010, **16**, 1232; (*d*) P. Wu, D. L. Ma, C. H. Leung, S. C. Yan, N. Zhu, R. Abagyan and C. M. Che, *Chem.–Eur. J.*, 2009, **15**, 13008; (*e*) M. R. Gill, J. Garcia-Lara, S. J. Foster, C. Smythe, G. Battaglia and J. A. Thomas, *Nat. Chem.*, 2009, **1**, 662; (*f*) J. Alzeer, B. R. Vummidi, P. J. C. Roth and N. W. Luedtke, *Angew. Chem., Int. Ed.*, 2009, **48**, 9362; (*g*) A. Membrino, M. Paramasivam, S. Cogoi, J. Alzeer, N. W. Luedtke and L. E. Xodo, *Chem. Commun.*, 2010, **46**, 625; (*h*) L. Xu, D. Zhang, J. Huang, M. Deng, M. Zhang and X. Zhou, *Chem. Commun.*, 2010, **46**, 743.

9 For recent reviews of G-quadruplex binders, see: (*a*) T. Ou, Y. Lu, Y. Tan, Z. Huang, K. Y. Wong and L. Gu, *ChemMedChem*, 2008, **3**, 690; (*b*) M. Franceschin, *Eur. J. Org. Chem.*, 2009, 2225.

10 (*a*) M. Tera, K. Iida, H. Ishizuka, M. Takagi, M. Suganuma, T. Doi, K. Shin-ya and K. Nagasawa, *ChemBioChem*, 2009, **10**, 431; (*b*) M. Tera, H. Ishizuka, M. Takagi, M. Suganuma, K. Shin-ya and K. Nagasawa, *Angew. Chem., Int. Ed.*, 2008, **47**, 5557; (*c*) M. Tera, Y. Sohtome, H. Ishizuka, T. Doi, M. Takagi, K. Shin-ya and K. Nagasawa, *Heterocycles*, 2006, **69**, 505.

11 Isolation of telomestatin, see: (*a*) K. Shin-ya, K. Wierzba, K. Matsuo, T. Ohtani, Y. Yamada, K. Furihata, Y. Hayakawa and H. Seto, *J. Am. Chem. Soc.*, 2001, **123**, 1262total synthesis of telomestatin, see; (*b*) T. Doi, M. Yoshida, K. Shin-ya and T. Takahashi, *Org. Lett.*, 2006, **8**, 4165.

12 For a recent review of the BODIPY dye, see: A. Loudet and K. Burgess, *Chem. Rev.*, 2007, **107**, 4891.

13 (*a*) R. Rodriguez, G. D. Pantos, D. P. N. Goncalves, J. K. M. Sanders and S. Balasubramanian, *Angew. Chem., Int. Ed.*, 2007, **46**, 5405; (*b*) L1H1-7OTD and L1A1-7OTD[10a] induced telo24 into antiparallel G-quadruplex in the presence or absence of KCl[10a].

14 (*a*) A. De Cian, L. Guittat, M. Kaiser, B. Sacca, S. Amrane, A. Bourdoncle, P. Alberti, M. P. Teulade-Fichou, L. Lacroix and J. L. Mergny, *Methods*, 2007, **42**, 183; (*b*) J. L. Mergny and J.-C. Maurizot, *ChemBioChem*, 2001, **2**, 124.

15 Stains-all® was used as a stain for non-specific single-stranded nucleotides which appear as red fluorescence ($\lambda_{ex}$ = 532 nm, 580-640 nm band pass filter).

16 No significant differences in $T_{1/2}$ values of double-stranded DNA in the presence nor absence of L1BOD-7OTD were observed (see ESI†).

17 (*a*) In the presence of the G-quadruplex ligand, telo24 (telomeric oligonucleotide) is in equilibrium with random structure and

 

G-quadruplex structure. Thus the G-quadruplex often appears as a smeared bands. See: M. Y. Kim, H. Vankayalapati, K. Shin-ya, K. Wierzba and L. H. Hurley, *J. Am. Chem. Soc.*, 2002, **124**, 2098; (*b*) To verify the interactions between the BODIPY fluorophore of **2** and the oligonucleotides, BODIPY **3** was used a control in electrophoresis experiments.

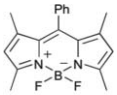


**3**

18 Part of the c-kit promoter region forms a four-looped parallel G-quadruplex, while in the case of bcl-2, a three-looped anti-parallel/parallel mixed structure is formed[1].

19 (*a*) F. Rosu, E. De Pauw and V. Gabelica, *Biochimie*, 2008, **90**, 1074; (*b*) K. Iida, M. Tera, T. Hirokawa, K. Shin-ya and K. Nagasawa, *Chem. Commun.*, 2009, 6481.

20 (*a*) J. A. Cruz-Aguado and G. Penner, *Anal. Chem.*, 2008, **80**, 8853; (*b*) D. C. Harris, X. Chu and J. Jayawickramarajah, *J. Am. Chem. Soc.*, 2008, **130**, 14950.

21 (*a*) The results of earlier ESI-MS analysis (see ESI†) suggest that L1BOD-7OTD (**2**) and GFOs form 1 : 1 and 1 : 2 complexes; (*b*) Since **2** bound to a GFO with two molecules, the concentration of apparent binding sites of GFO corresponded to 2-fold GFO concentration; (*c*) Since L1BOD-7OTD had low solubility in water, 50% DMSO was used for the FP titration assay system.

22 At the concentration of L1BOD-7OTD, the cells did not suffered acute cytotoxicity.

23 L1BOD-7OTD is presumed to be localized especially at nucleoli which is rich in single-stranded rDNA[8f,g].